Enzyme Inhibition

DOI: 10.1002/anie.201102967

Identification of Acyl Protein Thioesterases 1 and 2 as the Cellular Targets of the Ras-Signaling Modulators Palmostatin B and M

Marion Rusch, Tobias J. Zimmermann, Marco Bürger, Frank J. Dekker, Kristina Görmer, Gemma Triola, Andreas Brockmeyer, Petra Janning, Thomas Böttcher, Stephan A. Sieber, Ingrid R. Vetter, Christian Hedberg, and Herbert Waldmann**

The *S*-palmitoylated and *S*-farnesylated signal-transducing H- and N-Ras GTPases play important roles in cell growth, division, and differentiation, and are frequently mutated in melanoma, leukemia, and cancers of the bladder, liver, and kidney.[1–3]

Dynamic *S*-palmitoylation and *S*-depalmitoylation of H- and N-Ras by palmitoyl transferases and thioesterases determines proper Ras localization and signaling in cells.[4] Interference with the Ras-de/reacylation cycle by inhibition of the depalmitoylation through the use of the β-lactone acyl protein thioesterase 1 (APT1) inhibitors palmostatin B[5] or palmostatin M[6] (Figure 1) disturbs the precise H- and N-Ras steady-state localization, and results in down-regulation of global Ras signaling. Palmostatin B does not inhibit several phosphodiesterases with relevance to Ras signaling.[5] However, it remains unclear whether APT1 is the only Ras-depalmitoylating enzyme in cells and whether palmostatin B and M target additional proteins relevant to the Ras cycle, in particular the related isoenzyme APT2.[7]

Since the palmostatins are acylating reagents and, as in the case of APT1, inhibit their target proteins through reversible acylation of active-site nucleophiles,[5] their chemical nature offers an opportunity for the identification of the target by means of activity-based proteome profiling (ABPP) through slow reactive proteomics.[8,9] In ABPP, chemical probes with balanced reactivity are employed to tag, isolate, and identify enzyme targets on the basis of their mechanism of enzymatic catalysis. Typically, the reaction of a nucleophile in the enzyme active site with an electrophile embedded in a selective probe is employed. Previously, β-lactone-based probes have successfully been used to profile bacterial,[10,11] plant,[12] as well as mammalian proteomes.[13] A frequently applied strategy to facilitate target isolation by means of reactive proteomics is a bioorthogonal ligation of the covalently modified enzyme with an additional affinity tag, such as a suitably functionalized biotin. In particular, the copper(I)-catalyzed Huisgen [3+2] cycloaddition has served as an efficient tool for this purpose.[14,15]

Here we describe the development of ABPP probes based on the Ras depalmitoylation inhibitors palmostatin B[5] and M,[6] and the identification of APT1 and APT2 as their targets, which has relevance to the dynamic Ras palmitoylation cycle.

For target identification, we designed two ABPP probes based on our most potent compound palmostatin M (**1**) and the previously reported APT1 inhibitor palmostatin B (**2**). In the case of the probes based on **1**, an alkyne was introduced at the two sides of the molecule, thereby affording **3** and **4**, to facilitate isolation through a [3+2] cycloaddition (Scheme 1 A). For the synthesis of an ABPP probe derived from palmostatin B, the alkyne functionality was embedded in the lipid chain (**5**; Scheme 1 B; see the Supporting Information). This site previously served well for introduction of a fluorophore without compromising the inhibitory activity of APT1.[5] A conceptually similar strategy as for the synthesis of the focused β-lactone library in the development of palmostatin M[6] was employed and only the more potent *S*,*S* isomers were considered. In brief, an *anti*-aldol reaction between *O*-acylephedrine derivative **6** and aldehyde **7** resulted in the β-hydroxyester **8**. *S*-Oxidation of **8** with oxone, followed by saponification (LiOH) and subsequent β-lactonization with $PhSO_2Cl$ in pyridine yielded ABPP probe **3** (Scheme 1 C). The regioisomeric alkyne derivative **4** was synthesized in an analogous way by means of an *anti*-aldol reaction between *O*-dodecylated ephedrine derivative **9** and alkyne-aldehyde **10**, which led to the corresponding β-hydroxyester **11**, which was further transformed to **4** by β-lactonization with $PhSO_2Cl$ in pyridine (Scheme 1 D).

Investigation of APT1 inhibition by the ABPP probes with the established assay[6] revealed inhibition constants of $IC_{50} = 4.4$ nM for **3**, $IC_{50} = 10.0$ nM for **4**, and $IC_{50} = 6.0$ nM for **5**, which are in a similar range to the values reported for the corresponding non-alkyne-functionalized APT1 inhibitors. To

[*] Dipl.-Chem. M. Rusch, Dipl.-Chem. T. J. Zimmermann, M. Sc. M. Bürger, Dr. K. Görmer, Dr. G. Triola, A. Brockmeyer, Dr. P. Janning, Dr. I. R. Vetter, Dr. C. Hedberg, Prof. Dr. H. Waldmann
Max-Planck-Institut für Molekulare Physiologie
Abt. Chemische Biologie
Otto-Hahn-Strasse 11, 44227 Dortmund (Germany)
E-mail: christian.hedberg@mpi-dortmund.mpg.de
herbert.waldmann@mpi-dortmund.mpg.de
Dipl.-Chem. M. Rusch, Dipl.-Chem. T. J. Zimmermann, Dr. K. Görmer, Dr. G. Triola, A. Brockmeyer, Dr. P. Janning, Dr. C. Hedberg, Prof. Dr. H. Waldmann
Technische Universität Dortmund, Fakultät Chemie
Lehrbereich Chemische Biologie
Otto-Hahn-Strasse 6, 44227 Dortmund (Germany)
Dr. F. J. Dekker
Univ. of Groningen, University Centre for Pharmacy
A. Deusinglaan 1, 9713 AV Groningen (The Netherlands)
Dr. T. Böttcher, Prof. Dr. S. A. Sieber
Technische Universität München, Organic Chemistry II
Lichtenberg Strasse 4, 85747 Garching (Germany)

Supporting information for this article is available on the WWW under http://dx.doi.org/10.1002/anie.201102967.

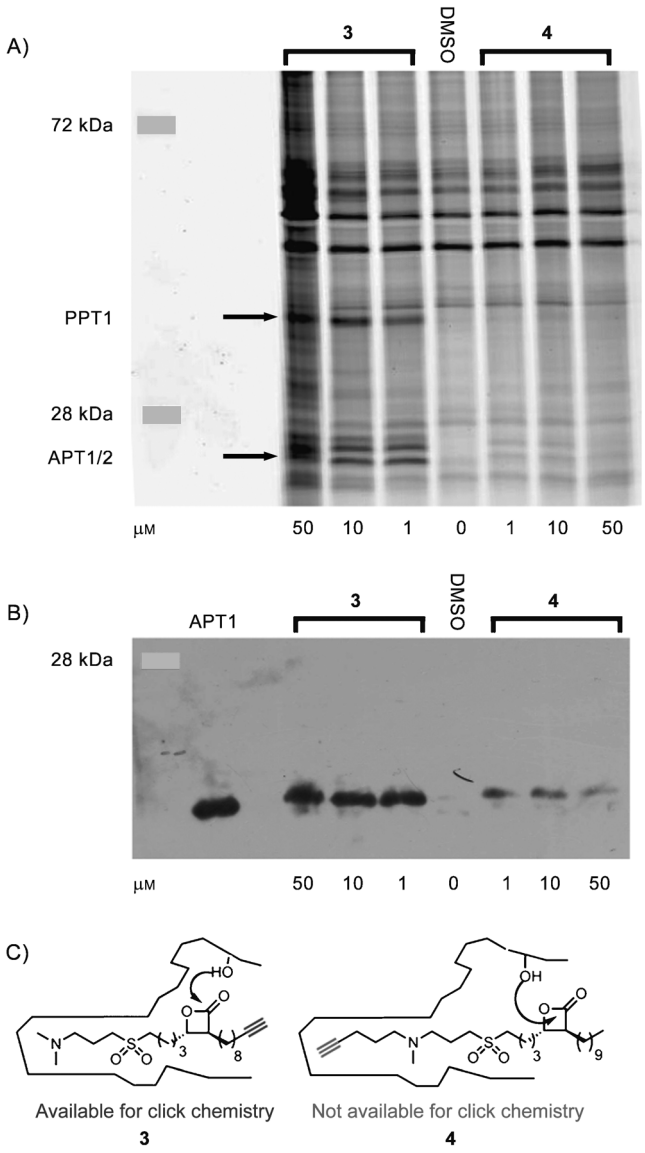

Figure 1. Cellular proteome labeling profile for probes **3** and **4** derived from palmostatin M after 20 min incubation at various probe concentrations (50, 10, 1 μM). A) Fluorescent gel highlighting three major bands corresponding to PPT1 (34.193 kDa), APT1 (MW = 24.67 kDa), and APT2 (MW = 24.73 kDa) Conditions: Biotin-rhodamine-N_3 = 20 μM, TCEP·HCl = 0.5 mM, ligand = 50 μM, $CuSO_4$ = 0.5 mM, HeLa cells = 2×10^6. B) Corresponding Western blot for APT1 visualization using polyclonal Rabbit APT1 antibody which shows a stronger affinity of probe **3** compared to **4** for APT1. Recombinant hAPT1 (25 ng) was used as the reference. C) Binding mode accounting for the observed APT1-labeling efficiency based on the accessibility of the alkyne group for the click reaction. TCEP = tris(2-carboxyethyl)phosphine.

characterize the protein targets of palmostatin M, HeLa cells were incubated with ABPP probes **3** and **4** at concentrations of 50 μM, 10 μM, and 1 μM. The cells were lysed and the labeled proteome was tagged by a copper-catalyzed [3+2] Huisgen reaction with an azide-biotin-rhodamine construct as previously described.[11] After enrichment on magnetic streptavidin beads, the bound proteins were released by heating and subjected to separation by sodium dodecylsulfate polyacrylamide gel electrophoresis (SDS-PAGE). In the case of incubation with ABPP probe **3**, in-gel fluorescence detection revealed three major fluorescent bands which are not present in the negative control (Figure 1 A). In the case of incubation with ABPP probe **4**, the labeling and identification of the bound proteins was found to be considerably less efficient (Figure 1 A). Excision of the bands, followed by in-gel tryptic digestion and subsequent identification of the proteins from the resulting peptide fragments by means of nano-HPLC MS/MS revealed the labeled proteins to be APT1, APT2, and with some probability, palmitoyl protein thioesterase 1[7,16] (PPT1). In addition, several other proteins were identified ($p < 0.01$, see the Supporting Information). According to current knowledge, none of these proteins display any enzymatic activity linked to Ras signaling. To gain insight into the efficiency of labeling by probes **3** and **4**, and thus their binding modes, we carried out a Western blot with a known amount of recombinant hAPT1 on a separate gel line (Figure 1 B). This blot allowed us to assess the total amount of APT1 pulled down with the two ABPP probes. Although, probes **3** and **4** display similar biochemical potency (IC_{50} = 4.4 nM and 10 nM, respectively), the pull-down efficiency significantly differs in terms of the amount of labeled APT1. This finding indicates that the alkyne in pull-down probe **3** is accessible for the dipolar cycloaddition and that the aminomethylsulfonyl group consequently penetrates the binding site, whereas the orientation might be reversed in the case of **4**, so that the alkyne is buried in the active site and no longer accessible (Figure 1 C). This difference in labeling is not only indicative of the binding mode of the probes, but also in accordance with their substrate-based design.[6]

Although palmostatin B and M display biochemical IC_{50} values in a similar range (5.4 and 2.5 nM, respectively), palmostatin M is several times more active in cells. To elucidate the cellular enzyme inhibition profile of palmostatin B versus palmostatin M, we subjected the alkyne-tagged analogue of palmostatin B (**5**) to analogous concentration-dependant affinity isolation experiments as compound **3** and analyzed the total amount of APT1 pulled down by Western blotting (Figure 2). Although the profiles of the fluorescent gels (Figure 2 A) were similar, quantification by Western blotting for APT1 showed detectable activity down to 50 nM for ABBP probe **3** derived from palmostatin M, whereas ABPP probe **5** derived from palmostatin B required a concentration of at least 100 nM to label detectable levels of APT1 under identical conditions (Figure 2 B).

Thus, the activity-based proteomic profiling identified only APT1 and APT2 as target proteins with potential relevance to Ras deacylation and signaling. APT2 has been suggested as a relevant thioesterase for Ras depalmitoylation before,[5,17] however, experimental proof has been lacking. To demonstrate that palmostatin M and B indeed inhibit APT2, and to explore differences in substrate specificity between the APTs, we expressed recombinant human APT2 protein in an analogous way as APT1.[6] To this end, the hAPT2 gene was Gateway-cloned into a pGEX expression vector and modified to contain a PreScission protease recognition sequence between the APT2 and the GST gene (for details and

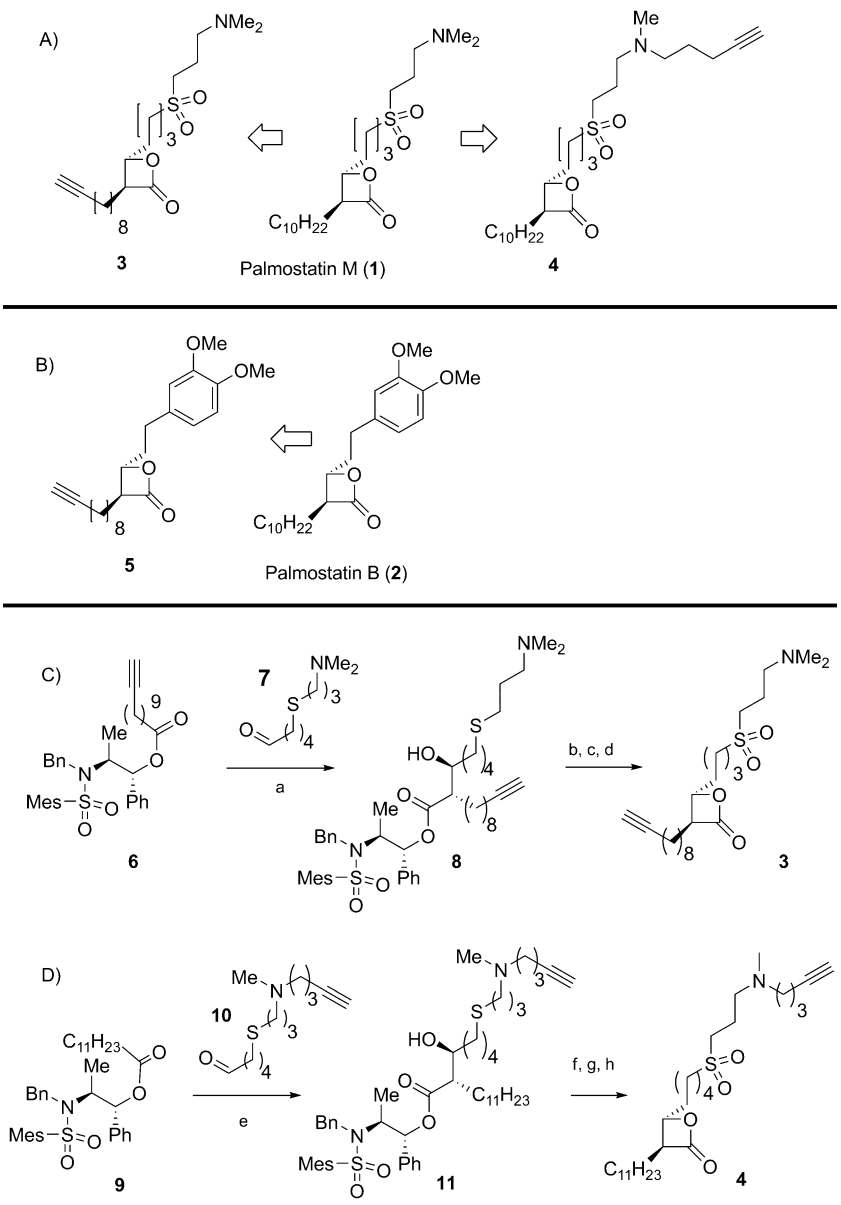

Scheme 1. A) Design of ABPP probes **3** and **4** derived from palmostatin M. B) Design of the ABPP probe **5** derived from palmostatin B. C) Synthesis of the β-lactone ABPP probe **3**: a) **6** (1.2 equiv), NEt_3 (2.5 equiv), $(CyHex)_2BOTf$ (2.2 equiv), −78 °C (2 h), CH_2Cl_2, 66%; b) oxone (3 equiv), RT (7 h), quantitative; c) LiOH (4 equiv), dioxane/H_2O (8:1), 40 °C, 2 days, 85%; d) $PhSO_2Cl$ (3 equiv), dry pyridine, 0 °C (24 h), 31%. D) Synthesis of the β-lactone ABPP probe **4**: e) **9** (1.2 equiv), NEt_3 (2.5 equiv), $(CyHex)_2BOTf$ (2.2 equiv), −78 °C (2 h), CH_2Cl_2, 40%; f) oxone (3 equiv), RT (7 h), 97%; g) LiOH (4 equiv), dioxane/H_2O (8:1), 40 °C, 2 days, 30%; h) $PhSO_2Cl$ (3 equiv), dry pyridine, 24 h, 0 °C, 30%. CyHex = cyclohexyl, OTf = trifluoromethanesulfonyl, Bn = benzyl, Mes = mesityl = 2,4,6-trimethylphenyl.

references see the Supporting Information). *Escherichia coli* BL21-CodonPlus(DE3)-RIL strain cells were transformed by the plasmid and expressed as GST fusion protein. After bacterial lysis, APT2 was separated from the GST by overnight incubation of the GSH column with PreScission protease. The resulting recombinant protein was purified to homogeneity by size-exclusion chromatography (see the Supporting Information). In general, 1.3 mg of protein was obtained from one liter of the bacterial culture. The DiFMUO-APT1 assay[6] was adjusted to monitor APT2 activity by correcting for the higher K_m value of the substrate (see the Supporting Information) and used to screen our focused β-lactone library. The IC_{50} values determined revealed a selectivity profile for APT2 very similar to that of APT1, with IC_{50} values being higher in general since the assay was performed at a higher enzyme concentration (50 nM for APT2 versus 5 nM for APT1). Sublibrary A is equally potent for inhibition of APT2 and APT1. Enzyme kinetic parameters for APT2 proved to be very similar to those of APT1, with a pre-steady-state inactivation rate higher than 4000 $mol^{-1}\,s^{-1}$. The inhibition mode was found to be of mixed mode (competitive-like) because of the slow rehydrolysis of the enzyme–inhibitor complex. None of the libraries A–C investigated could discriminate between APT1 and APT2, thus providing no opportunity to dissect APT1 from APT2 in the context of intracellular depalmitoylation events (Table 1).

APT1 has a broad substrate tolerance and in vitro deacylates several palmitoylated proteins, such as $G_{i\alpha1}$, eNOS, and H-Ras.[18–20] However, previous results showed that the catalytic efficiency of APT1 for $G_{i\alpha1}$ is threefold higher than for H-Ras, thus indicating some substrate preference for palmitoylated $G_{i\alpha1}$.[19] In agreement with this finding, studies carried out on yeast strains in which the APT1 gene was disrupted showed that the $G_{i\alpha1}$-depalmitoylating activity was completely abolished in these strains.[19] However, depalmitoylation of H-Ras was similar to that of wild-type strains, hence suggesting the existence of another depalmitoylating enzyme in yeast.[19] Although a direct equivalent for APT2 could not be found in yeast, it has been hypothesized that APT2 is a depalmitoylating enzyme with a different substrate preference than APT1.

To characterize APT2 and to gain novel insights into its possible involvement in Ras signaling we monitored the APT1- and APT2-mediated depalmitoylation of a biologically active semisynthetic N-Ras protein in vitro.[21] The palmitic acid liberated in the thioester hydrolysis was detected by means of the ADIFAB (acrylodated intestinal fatty acid binding protein) assay. ADIFAB is an established fluorescent indicator for the detection and measurement of free fatty acids.[22] Indeed, both APT1 and APT2 successfully depalmitoylate N-Ras in vitro at similar concentrations. Kinetic studies revealed comparable K_M values for both APT1 and APT2. Interestingly, the turnover number of

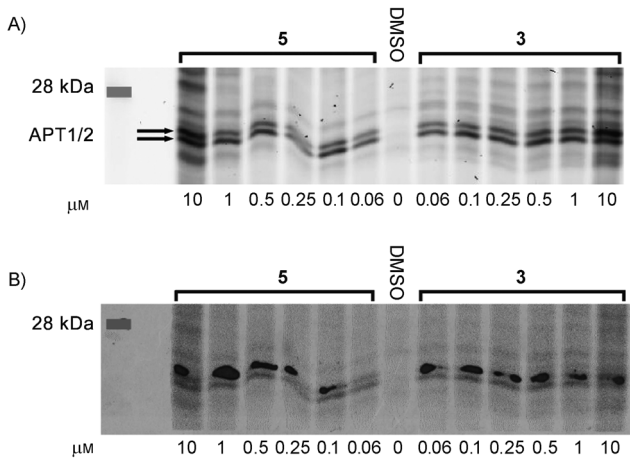

Figure 2. Concentration-dependent APT1 pull-down profile for probe **5** derived from palmostatin B and probe **3** derived from palmostatin M after 20 min incubation at probe concentrations ranging from 10 μM to 60 nM. A) Fluorescent gel highlighting the bands corresponding to APT1 (MW = 24.67 kDa) and APT2 (MW = 24.73 kDa). Conditions: Biotin-rhodamine-N_3 = 10 μM, TCEP·HCl = 0.5 mM, ligand = 50 μM, $CuSO_4$ = 0.5 mM, number of HeLa cells = 7×10^5. B) Corresponding Western blot for APT1 visualization (polyclonal Rabbit APT1 antibody) showing a stronger affinity of probe **3** than **5** for APT1.

Table 1: IC_{50} values for the inhibition of APT2 by focused β-lactone libraries A–C.

Compound (*S*,*S*)	IC_{50} APT2 [nM]	Compound (*R*,*R*)	IC_{50} APT2 [nM]
A 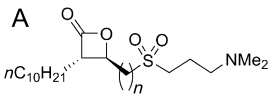		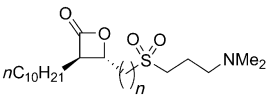	
12: *n* = 2	40.11 ± 4.87	**16**: *n* = 2	231.49 ± 16.19
13: *n* = 3	21.03 ± 0.65	**17**: *n* = 3	321.88 ± 28.69
14: *n* = 4	36.74 ± 2.35	**18**: *n* = 4	206.37 ± 22.01
15: *n* = 5	20.80 ± 1.24	**19**: *n* = 5	79.98 ± 5.30
B 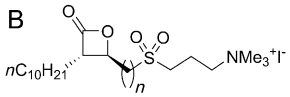		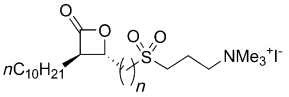	
20: *n* = 3	27.58 ± 1.64	**23**: *n* = 3	206.51 ± 13.15
21: *n* = 4	31.57 ± 2.02	**24**: *n* = 4	210.39 ± 15.21
22: *n* = 5	34.10 ± 3.50	**25**: *n* = 5	283.30 ± 27.22
C 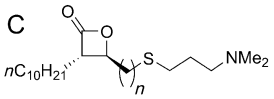		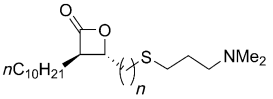	
26: *n* = 2	39.62 ± 3.17	**29**: *n* = 2	268.20 ± 13.44
27: *n* = 4	60.56 ± 15.25	**30**: *n* = 4	394.80 ± 60.61
28: *n* = 5	66.15 ± 3.89	**31**: *n* = 5	206.79 ± 17.03
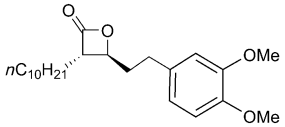		ABPP probes	
palm. B	19.58 ± 0.87	**3**:	32.44 ± 4.82
		4:	64.44 ± 7.13
		5:	23.72 ± 2.00

APT2 was double that of APT1 under identical conditions (Figure 3 and Table 2).

In conclusion, we have developed potent inhibitors of acyl protein thioesterases on the basis of substrate similarity

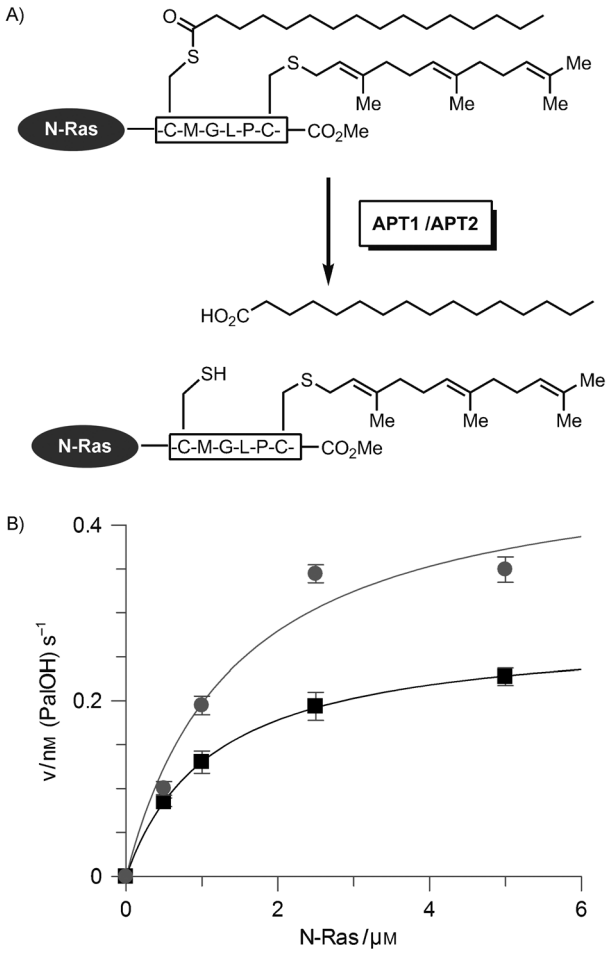

Figure 3. Deacylation of semisynthetic *S*-palmitoylated *S*-farnesyl-N-Ras by APT1 and APT2. A) APT1 and APT2 depalmitoylate semisynthetic N-Ras in vitro. B) Palmitoylated N-Ras was used at different concentrations as the substrate for APT1 (squares) and APT2 (circles). Reactions were initiated by addition of APT1 or APT2 (50 nM). Release of palmitic acid was followed by measuring the fluorescence spectra (400–650 nm) in the presence of 200 nM ADIFAB at room temperature. Fitted curves show the resulting palmitic acid detected versus time in each case.

Table 2: Kinetic parameters of the depalmitoylation of semisynthetic *S*-palmitoylated *S*-farnesyl-N-Ras with APT1 and APT2.

	K_M [μM]	K_{cat} [s^{-1}]	K_{cat}/K_M [$s^{-1}\,\mu M^{-1}$]
APT1	1.16 ± 0.015	5.62×10^{-3}	4.855×10^{-3}
APT2	1.43 ± 0.278	9.58×10^{-3}	6.693×10^{-3}

design principles and shown that they target APT1 and APT2 in cells. These inhibitors attenuate Ras signaling by interfering with the dynamic Ras de/reacylation cycle and induce phenotypic reversal of H-Ras-transformed cells.[6] Therefore, we suggest and provide a first experimental proof that both APT1 and APT2 are thioesterases relevant to Ras depalmitoylation and signaling. Notably, we could not identify other intracellular esterases (such as phospholipases A1, A2, C, and D) relevant to Ras signaling as targets for the palmostatins, which proves the selectivity of the probes. Taken together, these findings suggest that no further hydrolases employing a similar mechanism of catalysis, and possibly no further

hydrolases in general, are involved in Ras depalmitoyation in cells. For these reasons, inhibition of APT1 and APT2 may be a viable approach to interfere with H- and N-Ras signaling in malignant settings such as leukemia, melanoma, and bladder, liver, and kidney cancer.

Received: April 29, 2011
Revised: July 27, 2011
Published online: September 9, 2011

Keywords: acyl protein thioesterase · inhibition · proteomics · Ras proteins · signal transduction

[1] J. F. Hancock, *Nat. Rev. Mol. Cell Biol.* **2003**, *4*, 373 – 385.
[2] A. Wittinghofer, H. Waldmann, *Angew. Chem.* **2000**, *112*, 4360 – 4383.
[3] P. G. Dangle, B. Zaharieva, H. Jia, K. S. Pokar, *Recent Pat. Anti-Cancer Drug Discovery* **2009**, *4*, 125 – 136.
[4] O. Rocks, A. Peyker, M. Kahms, P. J. Verveer, C. Koerner, M. Lumbierres, J. Kuhlmann, H. Waldmann, A. Wittinghofer, P. I. H. Bastiaens, *Science* **2005**, *307*, 1746 – 1752.
[5] F. J. Dekker, O. Rocks, N. Vartak, S. Menninger, C. Hedberg, R. Balamurugan, S. Wetzel, S. Renner, M. Gerauer, B. Schoelermann, M. Rusch, J. W. Kramer, D. Rauh, G. W. Coates, L. Brunsveld, P. I. H. Bastiaens, H. Waldmann, *Nat. Chem. Biol.* **2010**, *6*, 449 – 456.
[6] C. Hedberg, F. Dekker, M. Rusch, S. Renner, S. Wetzel, N. Vartak, C. Geerding-Reimers, R. S. Bon, P. I. H. Bastiaens, H. Waldmann, *Angew. Chem.* **2011**, DOI: 10.1002/ange.201102965; *Angew. Chem. Int. Ed.* **2011**, DOI: 10.1002/anie.201102965.
[7] R. Zeidman, C. S. Jackson, A. I. Magee, *Mol. Membr. Biol.* **2009**, *26*, 32 – 41, and references therein.
[8] S. A. Sieber, B. F. Cravatt, *Chem. Commun.* **2006**, 2311 – 2319.
[9] M. J. Evans, B. F. Cravatt, *Chem. Rev.* **2006**, *106*, 3279 – 3301.
[10] T. Böttcher, S. A. Sieber, *J. Am. Chem. Soc.* **2008**, *130*, 14400 – 14401.
[11] T. Böttcher, S. A. Sieber, *Angew. Chem.* **2008**, *120*, 4677 – 4680; *Angew. Chem. Int. Ed.* **2008**, *47*, 4600 – 4603.
[12] Z. Wang, C. Gu, T. Colby, T. Shindo, R. Balamurugan, H. Waldmann, M. Kaiser, R. A. L. van der Hoorn, *Nat. Chem. Biol.* **2008**, *4*, 557 – 562.
[13] P.-Y. Yang, K. Liu, M. H. Ngai, M. J. Lear, M. R. Wenk, S. Q. Yao, *J. Am. Chem. Soc.* **2010**, *132*, 656 – 666.
[14] A. E. Speers, B. F. Cravatt, *Chem. Biol.* **2004**, *11*, 535 – 546.
[15] P. F. van Swieten, M. A. Leeuwenburgh, B. M. Kessler, H. S. Overkleeft, *Org. Biomol. Chem.* **2005**, *3*, 20 – 27.
[16] PPT1 is a lysosomal enzyme involved in the degradation of lipidated proteins, for details see J.-Y. Lu, S. L. Hofmann, *J. Lipid Res.* **2006**, *47*, 1352 – 1357. PPT1 is not considered relevant to Ras signaling due to its compartmental localization, although it has been shown that PPT1 depalmitoylates the Ras isoforms in biochemical assays, see L. Meng, N. Sin, C. M. Crews, *Biochemistry* **1998**, *37*, 10488 – 10492 and S. Cho, P. E. Dawson, G. Dawson, *J. Neurosci. Res.* **2000**, *59*, 32 – 38.
[17] Recently, APT2 was reported to specifically depalmitoylate GAP43 in cells, see V. M. Tomatis, A. Trenchi, G. A. Gomez, J. L. Daniotti, *PloS One* **2010**, 5, e15045.
[18] J. A. Duncan, A. G. Gilman, *J. Biol. Chem.* **1998**, *273*, 15830 – 15837.
[19] J. A. Duncan, A. G. Gilman, *J. Biol. Chem.* **2002**, *277*, 31740 – 31752.
[20] D. C. Yeh, J. A. Duncan, S. Yamashita, M. Michel, *J. Biol. Chem.* **1999**, *274*, 33148 – 33154.
[21] B. Bader, K. Kuhn, D. J. Owen, H. Waldmann, A. Wittinghofer, J. Kuhlmann, *Nature* **2000**, *403*, 223 – 226.
[22] G. V. Richieri, R. T. Ogata, A. M. Kleinfeld, *J. Biol. Chem.* **1992**, *267*, 23495 – 23501.

